CO$_2$ Capture by Absorption with Potassium Carbonate

Disclaimer

Abstract

The objective of this work is to improve the process for CO_2 capture by alkanolamine absorption/stripping by developing an alternative solvent, aqueous K_2CO_3 promoted by piperazine. A rigorous thermodynamic model has been developed with a stand-alone FORTRAN code to represent the CO_2 vapor pressure and speciation of the new solvent. Parameters have been developed for use of the electrolyte NRTL model in AspenPlus. Analytical methods have been developed using gas chromatography and ion chromatography. The heat exchangers for the pilot plant have been ordered.

Contents

Figures

Tables

Introduction

The objective of this work is to improve the process for CO_2 capture by alkanolamine absorption/stripping by developing an alternative solvent, aqueous K_2CO_3 promoted by piperazine. This work will expand on parallel bench scale work with system modeling and pilot plant measurements to demonstrate and quantify the solvent process concepts.

The bench-scale and modeling work is supervised by Gary Rochelle. Frank Seibert is supervising the pilot plant. Two students supported by the Texas Advanced Technology Program (Tim Cullinane and Marcus Hilliard) have made contributions this quarter to the scope of this project. Two new graduate students (Babatunde Oyenekan and Eric Chen) were recruited to start work with DOE support in January 2003 for direct effort on the scope of this contract. One student (Terraun Jones) has been supported by industrial funding.

Experimental

The following sections of this report detail experimental methods:

Subtask 2.1 (Pilot plant test plan) describes methods for piperazine analysis by gas and ion chromatography.

Subtask 2.2 (Design, Modifications, Order Equipment and Packing Materials) describes details in the design and modification of the pilot plant for future testing.

Results and Discussion

Progress has been made on four subtasks in this quarter:

Subtask 1.1 – Modify Vapor-Liquid Equilibrium (VLE) Model

The stand-alone FORTRAN model has been applied by Tim Cullinane to thermodynamic data for CO_2/water/potassium carbonate/piperazine. Work with the electrolyte- electrolyte non-random two-liquid (NRTL) model in AspenPlus has been initiated by Marcus Hilliard.

Subtask 1.3 – Develop Integrated Absorber/Stripper Model

Babatunde Oyenekan initiated development of an integrated stripper model.

Subtask 2.1 – Pilot Plant Test Plan

Terraun Jones developed analytical methods for piperazine and potassium using gas chromatography and ion chromatography.

Subtask 2.2 - Design, Modifications, Order Equipment and Packing Materials

Eric Chen has developed a detailed schedule for modifying the pilot plant. The air cooler and solvent cooler have been ordered. Exchangers to be used as the solvent heater have been received from Huntsman Chemical.

Conclusions

1. Measurements of speciation in piperazine-promoted potassium carbonate can be regressed by a the stand-alone NRTL electrolyte model with an average error of about 5%.
2. The partial molal heat capacity of piperazine anions can be highly negative.
3. Aspen Custom Modeler should be a more flexible numerical framework for simulating stripper performance that RateFrac.
4. The rate of oxidative degradation of piperazine appears to be about the same as that of MEA.
5. The absorber stripper pilot plant should start shakedown in November 2003.

Future Work

We expect the following accomplishments in the next quarter:

Subtask 1.1 – Modify Vapor-Liquid Equlibrium (VLE) Model

Initial results will be obtained with the electrolyte-NRTL model in Aspen Plus.

Subtask 1.3 – Develop Integrated Absorber/Stripper Model

A preliminary stripper model will be implemented in Aspen Custom Modeler.

Subtask 2.1 – Pilot Plant Test Plan

A detailed test plan will be developed for the first campaign.

Subtask 2.2 - Design, Modifications, Order Equipment and Packing Materials

All of the equipment and materials will be ordered for the pilot plant modifications. The welding package will be released for bidding.

Task 1 – Modeling Performance of Absorption/Stripping of CO_2 with Aqueous K_2CO_3 Promoted by Piperazine

Subtask 1.1a – Modify Vapor-Liquid Equlibrium (VLE) Model – Stand-alone FORTRAN Model

by J. Tim Cullinane

The work presented here is the continuing development of aqueous potassium carbonate/piperazine mixtures for CO_2 removal from flue gas. Previously, data on CO_2 partial pressure, piperazine speciation, and CO_2 absorption rates was collected (Cullinane, 2002). A rigorous thermodynamic model is now being developed to predict the equilibrium and speciation in potassium carbonate/piperazine mixtures for future use in process and kinetic modeling. The model, taken from previous work by Austgen (1989) and Posey (1996), utilizes the electrolyte NRTL model (Chen et al., 1982) to estimate activity coefficients and solve the necessary equilibrium expressions.

Equilibrium Modeling

Previous work in modeling the potassium carbonate/piperazine mixtures focused on the development of a simple model to describe equilibrium behavior (Cullinane, 2002). A simple model is capable of approximating the behavior of the system, but a more thermodynamically rigorous model is desirable for describing the complex solution characteristics for future use in rate and process models.

The thermodynamic model selected for the solutions is the electrolyte NRTL developed by Chen et al. (1982). The model uses binary interaction parameters, τ, to represent the impact of a molecule or ion on excess Gibbs free energy. The binary interaction can be represented as

$$\tau_{ji} = \frac{g_{ji} - g_{ii}}{RT}$$

where i and j represent differing species. The electrolyte NRTL uses three terms to model the excess Gibbs energy. The first, the Pitzer-Debye-Huckel term, is a long-range contribution to describe ion-ion interactions at low concentrations. The second term, the Born correction, accounts for changes in the dielectric constant of the solution as the solvent reference state changes. Finally, short-range contributions, dominant at high concentrations, are represented by the NRTL model (Renon and Prausnitz, 1968). The excess Gibbs energy of the three terms can be added to arrive at a total excess Gibbs energy for each term.

$$\frac{g_{ex}^*}{RT} = \frac{g_{ex\,PDH}^*}{RT} + \frac{g_{ex\,Born}^*}{RT} + \frac{g_{ex\,NRTL}^*}{RT}$$

The excess free energy is related to the activity coefficient by the following thermodynamic relationship.

$$\ln \gamma_i = \frac{g_{ex}^*}{RT}$$

In the model used in this work, all molecule-molecule and ion pair-ion pair parameters are set to zero. All acid gas-ion pair and ion pair-acid gas parameters, and molecule-ion pair and ion pair-molecule parameters not regressed were fixed at values of 15 and –8 respectively. Non-regressed water-ion pair and ion pair-water parameters were fixed at values of 8 and –4. Also, all τ's are assumed to have no temperature dependence unless otherwise specified. Henry's constant of CO_2 is assumed to be that of CO_2 in water. Equilibrium constants used are those found in Posey (1996) and Bishnoi (2000). A more thorough discussion of electrolyte NRTL theory as it pertains to gas treating solvents can be found in Austgen (1989) and Posey (1996).

To develop a working model of potassium carbonate/piperazine mixtures, τ must be found for significant contributing species. To simplify the analysis, τ's will be regressed sequentially for several independent data sets to reduce the number of simultaneously regressed parameters. The form used for binary interaction parameters is

$$\tau = A + B \cdot \left(\frac{1}{T} - \frac{1}{353.15} \right)$$

The sequence and the regressed parameters are shown in Table 1. After each step, parameter values were fixed at the regressed values for the remainder of the sequence to maintain a thermodynamically consistent model.

Table 1. Regressed Binary Interaction Parameters for the Electrolyte NRTL Model

	$\tau_{i,jk}$ or $\tau_{ij,k}$			$\tau = A + B(1/T - 1/353.15)$				
Step	**i**	**j**	**k**	**A**	σ_A	**B**	σ_B	**τ, 298K**
1	H_2O	K^+	CO_3^{2-}	8.652	0.162	860.9	371.1	**9.102**
	K^+	CO_3^{2-}	H_2O	-4.304	0.033	-215.9	74.6	**-4.417**
2	H_2O	K^+	HCO_3^-	6.722	0.039	1614.2	153.4	**7.565**
	K^+	HCO_3^-	H_2O	-3.001	Indet.*.	-122.0	Indet.*	**-3.064**
3	H_2O	PZH^+	HCO_3^-	8.315	0.158	Def.**	-	**8.315**
	H_2O	PZH^+	$PZCOO^-$	6.093	3.883	8840.1	5200.4	**10.711**
	PZH^+	$PZCOO^-$	H_2O	-5.306	0.813	Def.**	-	**-5.306**
	H_2O	PZH^+	$PZ(COO^-)_2$	5.010	0.426	Def.**	-	**5.010**
	PZ	PZH^+	$PZCOO^-$	Def.**	-	-9210.2	13219.0	**10.189**
	PZH^+	$PZCOO^-$	PZ	-12.506	3.085	Def.**	-	**-12.506**
	CO_2	PZH^+	HCO_3^-	7.168	1.259	Def.**	-	**7.168**

4	$\tau_{i,jk}$ or $\tau_{ij,k}$			$\tau = A + B(1/T-1/353.15)$				
	H_2O	K^+	$PZCOO^-$	10.594	0.737	-27297.3	6428.8	**-3.665**
	K^+	$PZCOO^-$	H_2O	-2.479	0.205	Def.**	-	**-2.479**
	H_2O	K^+	$PZ(COO^-)_2$	4.369	4.095	-25859.4	22296.0	**-9.134**

* Indeterminate: Represents a high correlation between Step 2 parameters.
** Default parameters used.

The regression of parameters is accomplished using a non-linear regression package called GREG (Caracotsios, 1986). Experimental or known values are compared to values predicted by the model. In an iterative process, user defined parameters are adjusted until the least squares difference of these values is minimized.

First, model parameters were adjusted to fit data for the activity of water in K_2CO_3-water mixtures as calculated from freezing point depression, and boiling point elevation and vapor pressure reported by CRC (2000) and Aseyev (1999) respectively. The data provides a wide range of both temperature (235 to 393 K) and concentration (0.0 to 50 wt% K_2CO_3). The values of four regressed parameters as well as their standard deviations are shown in Table 1 and are consistent with other salt solutions as reported by Chen et al. (1982). With the regressed parameters, the model predicts the activity coefficient of water within 2% of the values given in the literature.

The second set of regressed parameters describes $KHCO_3$ behavior as interpreted from VLE data by Tosh et al. (1959). The values of the regressed parameters are also reported in Table 1. A normalized parity plot of the predicted CO_2 partial pressures is shown in Figure. The figure shows a large degree of scatter among the data points. Within the spread, it appears that predictions of 20 wt% K_2CO_3 are centered lower than experimental values, predictions of 30 wt% K_2CO_3 agree with experimental data, and predictions of 40 wt% K_2CO_3 are centered higher than expected. This may be due to the experimental method used in the study. Or, a failure of the model to predict concentration effects on the temperature dependence may be to blame. Regardless, most points are predictable to within 20%.
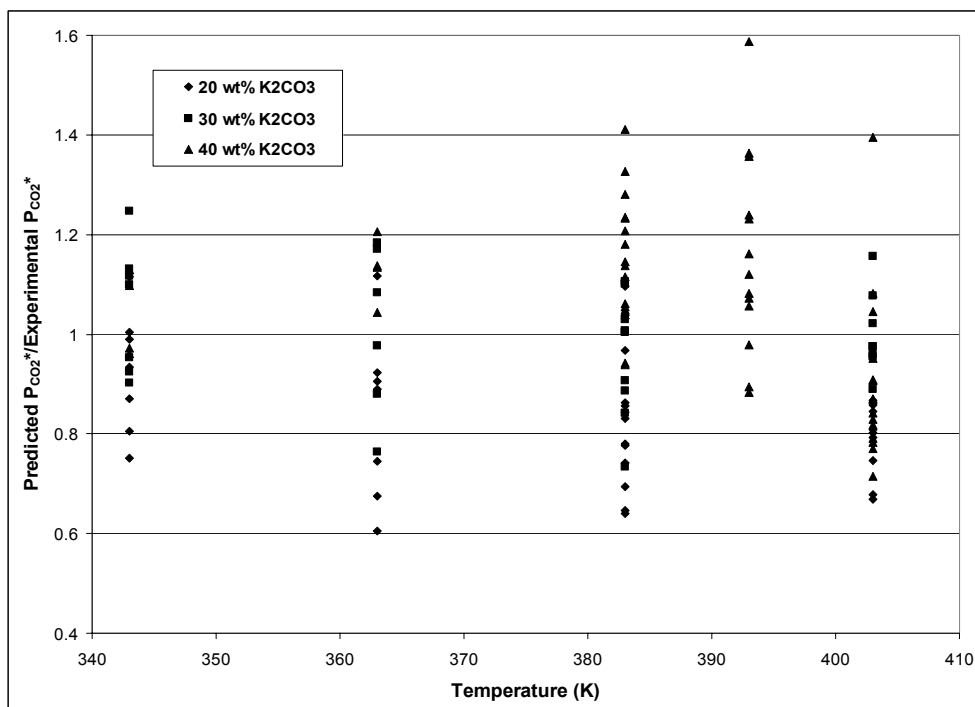
Figure 1. Electrolyte NRTL Model Predictions of CO₂ Vapor Pressure in Aqueous Potassium Carbonate Solutions (Tosh et al., 1959) Using Parameters Shown in Table 1

Proton (^{1}H) NMR data on the speciation of loaded piperazine solutions as well as total pressure data over such solutions are reported by Kamps *et al*. (2002) and Ermatchkov *et al*. (2002). Additional vapor pressure data was found in Bishnoi (2000). This data was used to regress the τ's necessary to describe the contribution of piperazine species to activity. The binary interaction parameters are shown in Table 1. Equilibrium constants for three reactions were simultaneously taken from Bishnoi (2000) for the following reactions.

$$PZH^+ + H_2O \longleftrightarrow PZ + H_3O^+$$

$$PZCOO^- + CO_2 + H_2O \longleftrightarrow PZ(COO^-)_2 + H_3O^+$$

$$H^+PZCOO^- + H_2O \longleftrightarrow PZCOO^- + H_3O^+$$
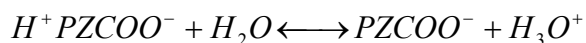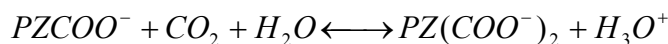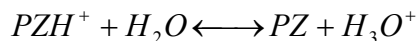
The model predictions are shown in Figures 2 and 3. The relative error of prediction is highest for PZ(COO⁻)₂ because it is present in small quantities in comparison to PZ or PZCOO⁻. Regardless, the model is capable of predicting speciation within an absolute error of 5%.
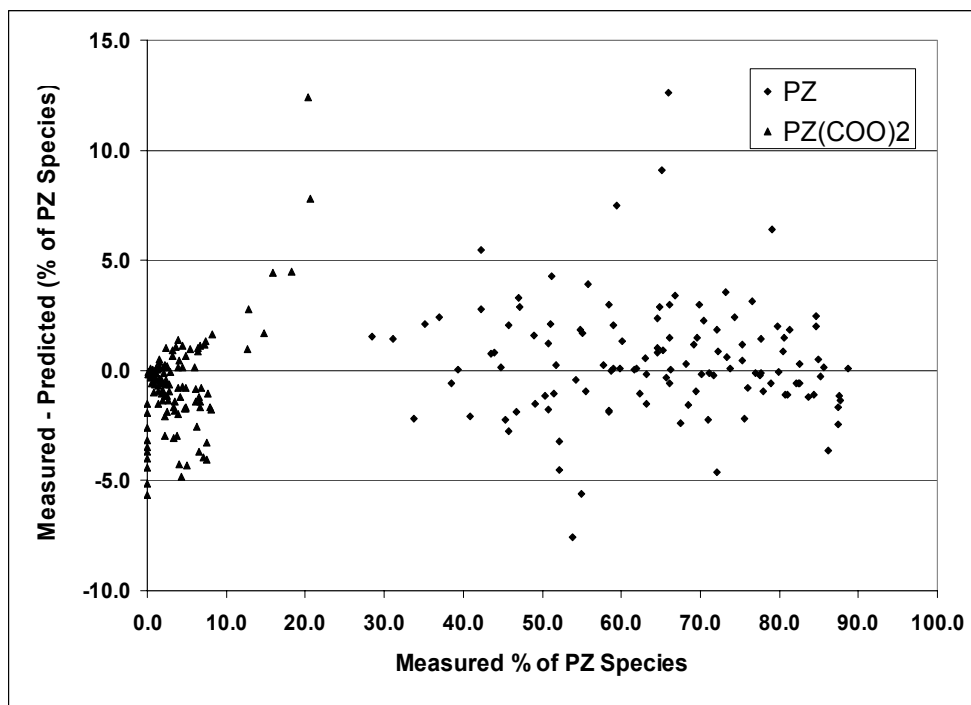
Figure 2. Absolute Error of Model Predictions of Piperazine Speciation as Given in Ermatchkov et al. (2002)

The final regression in the sequence utilized past (Cullinane, 2002) and current ^{1}H NMR data on the speciation of loaded aqueous piperazine in the presence of potassium carbonate to obtain parameters describing potassium and piperazine interactions. The resulting parameters are shown in Table 1 and the predictions are displayed in Figure 3. Throughout the range of concentration and loading, the model demonstrates its versatility and accuracy of correctly predicting the speciation.
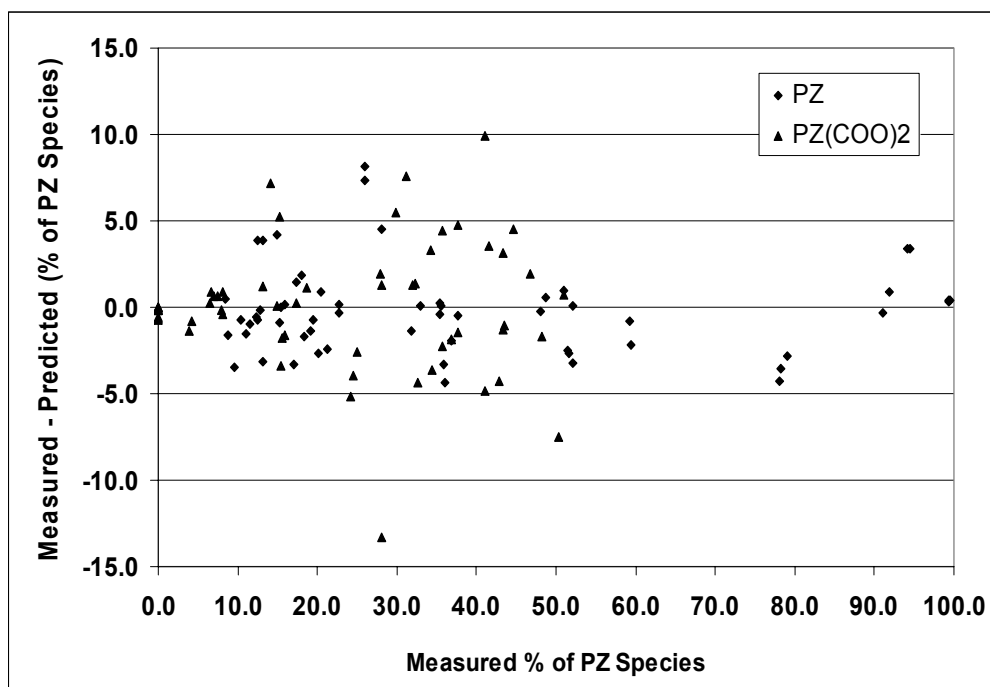
Figure 3. Absolute Error of Model Predictions of Potassium/Piperazine Speciation (Cullinane, 2002)

Using the model, speciation predictions were made in two solutions: 0.6 m PZ (Figure 4) and 3.6 m K+/0.6 m PZ (Figure 5). In the absence of potassium carbonate, piperazine is much more susceptible to protonation from the addition of CO_2 to the system. Model predictions show that protonated piperazine is the dominant species at $P_{CO2}* > 250$ Pa. This is significant due to the decreased amount of free amine available for reaction with CO_2, potentially detracting from the rate of CO_2 absorption.

In contrast, the 3.6 m K^+/0.6 m PZ solution contains much more of the carbamated species. Because piperazine carbamate is still reacts with CO_2, this solution maintains a fast absorption rate. The carbonate successfully buffers the solution at a higher pH, preventing the protonation, and thus the loss, of reactive piperazine.

Future work with the model will require accurate predictions of VLE of various solutions. Parameters affecting the activity of CO_2 in solution will be regressed to fit partial pressure and total pressure data available for systems containing piperazine and potassium carbonate. These parameters will be coordinated with previously regressed parameters to redefine the speciation. Also, the model will be coupled with a rigorous rate code (Bishnoi, 2000). Together the models will be used to regress kinetic parameters for modeling the absorption of CO_2 into K^+/PZ mixtures.
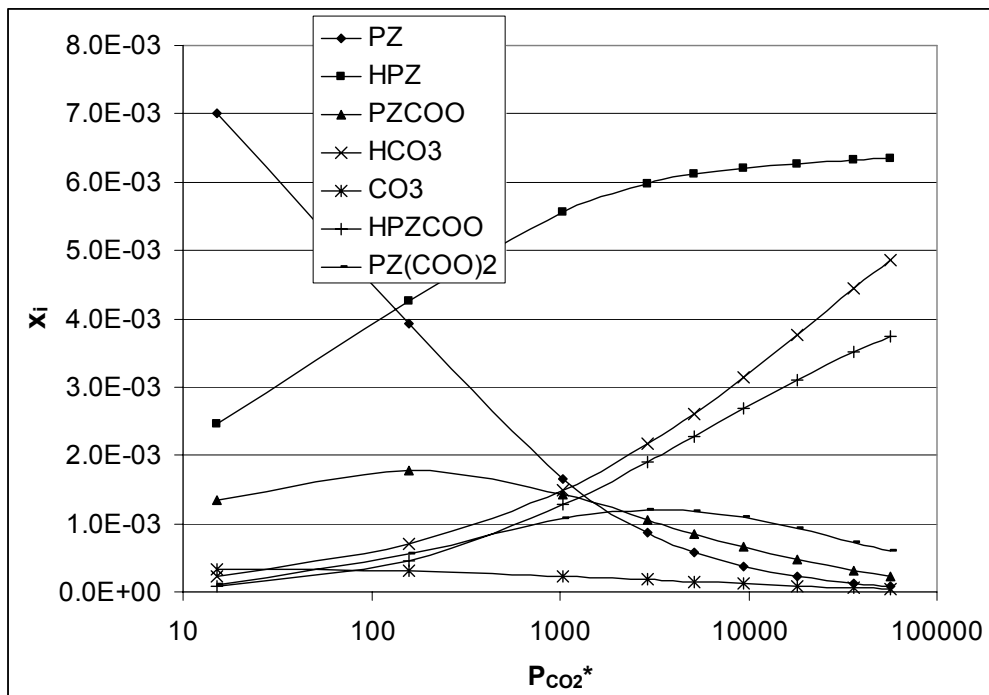
Figure 4. Speciation in 0.6 m PZ at 333 K
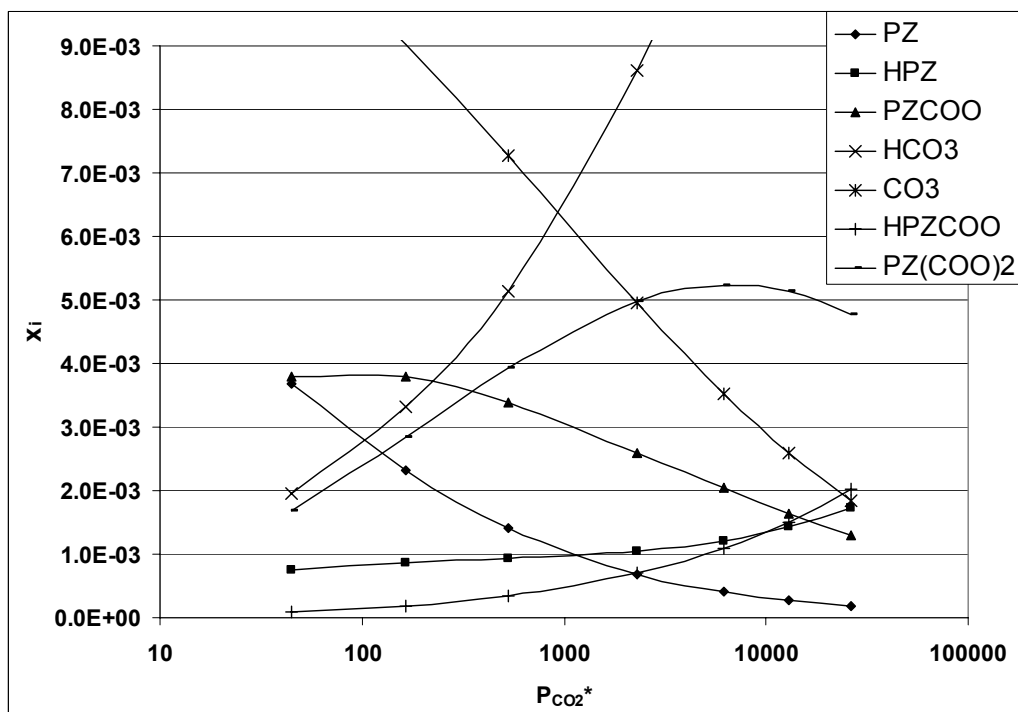
Figure 5. Speciation in 3.6 m K+/0.6 m PZ at 333 K

<u>Subtask 1.1b – Modify Vapor-Liquid Equilibrium (VLE) Model – Aspen Plus</u>

by Marcus Hilliard
(Supported by this contract)

      The objective of this subtask is to develop an NRTL thermodynamic model of piperazine/K_2CO_3 solvent for use in an Aspen Plus™ model of the absorption/stripping process. The model, which should predict the speciation and vapor pressure of carbon dioxide solvent composition and temperature, will be implemented in Aspen Plus™ to facilitate use of previous models in the integrated simulation. In this reporting period, we have developed the basic property data for piperazine species
(PZH^+ , $PZCOO^-$, H^+PZCOO^- , $PZ(COO^-)_2^{-2}$) that are not in the Aspen Plus™ database.

Discussion

      For potassium carbonate with piperazine, Cullinane (2002) expanded a simple equilibrium model for monoethanolamine with piperazine to include the impact of potassium ion for the following system:

$$CO_2(aq) + 2 \cdot H_2O \leftrightarrow HCO_3^- + H_3O^+ \tag{1}$$
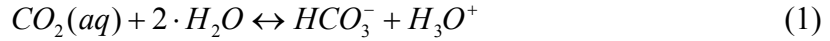
$$K_{HCO_3^-} = \frac{x_{HCO_3^-} \cdot x_{H_3O^+}}{x_{CO_2} \cdot x_{H_2O}^2} \tag{2}$$

$$HCO_3^- + H_2O \leftrightarrow CO_3^{-2} + H_3O^+ \tag{3}$$
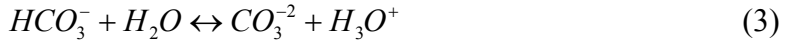
$$K_{CO_3^{2-}} = \frac{x_{H_3O^+} \cdot x_{CO_3^{2-}}}{x_{HCO_3^-} \cdot x_{H_2O}} \tag{4}$$

$$2 \cdot H_2O \leftrightarrow H_3O^+ + OH^- \tag{5}$$

$$K_W = \frac{x_{H_3O^+} \cdot x_{OH^-}}{x_{H_2O}^2} \tag{6}$$

$$PZH^+ + H_2O \leftrightarrow PZ + H_3O^+ \tag{7}$$

$$K_{PZH+} = \frac{x_{PZ} \cdot x_{H_3O^+}}{x_{PZH^+} \cdot x_{H_2O}} \tag{8}$$

$$PZ + CO_2 + H_2O \leftrightarrow PZCOO^- + H_3O^+ \qquad (9)$$
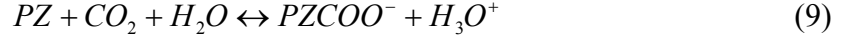
$$K_{PZCOO^-} = \frac{x_{PZCOO^-} \cdot x_{H_3O^+}}{x_{PZ} \cdot x_{CO_2} \cdot x_{H_2O}} \qquad (10)$$

$$H^+PZCOO^- + H_2O \leftrightarrow PZCOO^- + H_3O^+ \qquad (11)$$
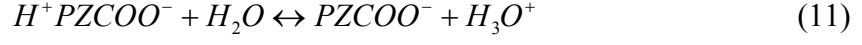
$$K_{H^+PZCOO^-} = \frac{x_{PZCOO^-} \cdot x_{H_3O^+}}{x_{H^+PZCOO^-} \cdot x_{H_2O}} \qquad (12)$$

$$PZCOO^- + CO_2 + H_2O \leftrightarrow PZ(COO^-)_2 + H_3O^+ \qquad (13)$$

$$K_{PZ(COO^-)^2} = \frac{x_{PZ(COO^-)_2} \cdot x_{H_3O^+}}{x_{PZCOO^-} \cdot x_{CO_2} \cdot x_{H_2O}} \qquad (14)$$

where

PZH^+ = Protonated Piperazine

$PZCOO^-$ = Piperazine Carbamate

H^+PZCOO^- = Protonated Piperazine Carbamate

$PZ(COO^-)_2^{-2}$ = Piperazine Bicarbamate

Table 2. Equilibrium Constants

$$\ln K_i = A + B / T + C \ln T$$

Equation #	A	B	C
2	231.4	-12092	-36.78[A]
4	216	-12432	-35.48[A]
6	132.9	-13446	-22.48[A]
8	-11.91	-4351	None[B]
10	-29.31	5615	None[C]
12	-8.21	-5286	None[C]
14	-30.78	5615	None[C]

Sources: A- Edwards et al. (1978), Posey (1996); B- Pagano et al. (1961); C- Bishnoi (2000)

Cullinane (2002) then assembled equilibrium constants for the above reactions as a function of temperature determined by Edwards et al. (1978), Posey (1996), Pagano et al. (1961), and Bishnoi (2000). Please refer to Table 2 above for more information.

For this work, we have chosen to use the electrolyte-NRTL activity coefficient method (ELECNRTL). According to Aspen Technology (2001a), "ELECNRTL model can represent aqueous and aqueous/organic electrolyte systems over the entire range of electrolyte concentrations with a single set of binary interaction parameters". Aspen Plus[TM] Physical Property Databanks can retrieve most pure component property parameters, but for electrolyte systems it becomes necessary to supply Aspen with missing data. Table 3 shows the parameter requirements for the ELECNRTL property method.

Table 3. Parameters Required for the ELECNRTL Property Method

Thermodynamic Properties	Models	Parameter Requirements
Vapor mixtures		
Fugacity coefficient, Density,	Redlich-Kwong	TC, PC
Enthalpy, Entropy, Gibbs energy	Ideal gas heat capacity/ DIPPR/ Barin correlation	CPIG or CPIGDP or CPIXP1, CPIXP2, CPIXP3
Liquid mixture		
Fugacity coefficient, Gibbs energy	Electrolyte NRTL	Molecule (Mol.): CPDIEC Ion: RADIUS Mol.-Mol.: NRTL Mol.-Ion, Ion-Ion: GMELCC, GMELCD, GMELCE, GMELCN
	Extended Antoine vapor pressure	PLXANT
	Henry's constant	Solvent: VC, Mol. Solute-solvent HENRY
	Brelvi-O'Connell	Solvent: TC, PC, (ZN or RKTZRA), Mol. solute: (VC or VLBROC)
Enthalpy, Entropy	Ideal gas heat capacity/ DIPPR and	CPIG or CPIGDP
	Watson/ DIPPR heat of vaporization	Solvent: TC, (DHVLWT or DHVLDP)
	Infinite dilution heat capacity/ Criss-Cobble	Ions: CPAQ0 or Ions: IONTYP, S025C
	Electrolyte NRTL	Mol.: CPDIECC Ion: RADIUS Mol.-Mol.: NRTL Mol.-Ion, Ion-Ion: GMELCC, GMELCD, GMELCE, GMELCN
Density	Rackett/Clarke	Mol.: TC, PC, (VC or VCRKT), (ZC or RKTZRA) Ion-ion: VLCLK

Source: Criss and Cobble (1964a)

For a complete list of scalar and temperature dependent parameter nomenclature, please refer to Appendix A.

For ions, Aspen Physical Property System, by default, assumes the following scalar physical property quantities listed in Table 4.

Table 4. Default Scalar Parameters for the ELECNRTL Property Method

Property	Units	Default Value
API		0
CHI		0
DGFVK		0
DGSFRM	kcal/mol	0
DHFVK	kcal/mol	0
DHSFRM	kcal/mol	0
MUP	debye	0
DLWC		1
DVBLNC		1
HCOM		0
OMEGA		0.296
PC	bar	29.6882
RADIUS	m	3.00E-10
RHOM		0
RKTZRA		0.25
TB	°C	68.75
TC	°C	234.25
TFP	°C	-95.35
TREFHS		25
VB	cc/mol	140.903
VC	cc/mol	369.445
VCRKT		250
VLSTD	cc/mol	0
ZC		0.26

Source: Aspen Technology (2001b).

For a complete list of scalar parameter nomenclature, please refer to Appendix A. Table 5 lists the scalar parameters Aspen Plus^{TM} requires to describe a molecule/ion.

Table 5. Molecule/Ion Scalar Parameters for the ELECNRTL Property Method

Property	Units
CHARGE	
DGAQFM	
DGAQHG	
DGFORM	kcal/mol
DHAQFM	
DHAQHG	
DHFORM	kcal/mol
IONRDL	
MW	
OMEGHG	
S25HG	cal/mol-K
S025C	cal/mol-K
S025E	cal/mol-K

Source: Aspen Technology (2001b).

If the estimation methods are available, Aspen Physical Property System can estimate some scalar parameters required by the physical property model, but the application range for each method, and the expected error for each method varies. This worked focused on estimating the partial molar entropy at infinite dilution (S025C) for piperazine ionic constituents (PZH^+ , $PZCOO^-$, H^+PZCOO^- , $PZ(COO^-)_2^{-2}$) from correlations of the ionic charge, radius, and structure of the ionic species to other thermodynamic properties (i.e., aqueous heat capacity at infinite dilution and the aqueous enthalpy of formation at infinite dilution). These types of calculations are beyond the scope of Aspen Physical Property System capabilities.

Entropy Estimation Techniques

Due to the nature of entropy, an experimental method to measure entropy for individual ions at infinite dilution is unavailable. Therefore, researchers assign an arbitrary value or reference state to the concentration of the hydrogen ion ($\bar{S}_{H^+}^\circ$ = -5.5 cal mol^{-1} K^{-1}, absolute scale; 0.0 cal mol^{-1} K^{-1}, relative scale) and then calculate corresponding values for various ions. Horvath (1985) assembled the results that researchers have made for the estimation and correlation methods of entropy. Horvath described the results published by Powell and Latimer in 1951, who proposed the following correlation for the estimation of entropy ($\bar{S}_j^\circ$) of a monatomic ion as a function of the molecular weight (M_j) of the ion, charge of the ion (z), and effective ionic radius (r_e), ($\bar{S}_{H^+}^\circ$ = 0.0 cal mol^{-1} K^{-1}):

$$\bar{S}_j^\circ = \frac{3}{2} R \log M_j + 37.0 - \frac{270 \cdot z}{r_e^2} \qquad (15)$$

Wulff (1967) and Cox and Parker (1973) reported that the correlation developed by Powell and Latimer represented published values within 2-3 cal mol^{-1} K^{-1}. Laidler (1957) suggested that Powell and Latimer's relation did not take into account Born's theory for entropy changes for reactions of various ionic types and proposed a correlation for the entropy of an ion at infinite dilution as a function of the square of the ionic charge and the univalent radii. Laidler then used the method of least squares to develop the following correlation for estimating the entropy of monatomic ions ($\bar{S}^{\circ}_{H^+}$ = 0.0 cal mol^{-1} K^{-1}):

$$\bar{S}^{\circ}_j = \frac{3}{2} R \log M_j + 10.2 - \frac{11.6 \cdot z^2}{r_u} \tag{16}$$

Scott and Hugus (1957) confirmed equivalent nature of the expressions developed by Powell and Latimer and later by Latimer. King (1959) then concluded that such a relationship did not provide the rigorous solutions to accurately describe the partial molar entropy at infinite dilution. King did suggest that the expressions adequately described the relationships of ions in aqueous solutions.

Criss and Cobble (1964a,b) introduced the correspondence principle to accurately predict elevated temperature thermodynamic properties, thus avoiding the need for experimental measurements. They summarized the correspondence principle as follows:

> A standard state can be chosen at every temperature such that the partial molar entropies of one class of ions at that temperature are linearly related to the corresponding entropies at some reference temperature (Criss and Cobble, 1964a,b).

In other words, the correspondence principle suggested that the ionic entropies at an elevated temperature are linearly related to the corresponding entropy at 25°C ($\bar{S}^{\circ}_{H^+}$ = -5.0 cal mol^{-1} K^{-1}):

$$\bar{S}^{\circ}_t = a(t) + b(t) \cdot \bar{S}^{\circ}_{25}(abs.) \tag{17}$$

where

$\bar{S}^{\circ}_{25}(abs.)$ = absolute reference partial molar entropy at 25°C,

$a(t), b(t)$ = entropy coefficients (Simple cations, Na+; simple anions, OH-; oxy anions; acid oxy anions; and H+) at various temperatures.

To convert to the relative scale:

$$\bar{S}^{\circ}_{25}(abs.) = \bar{S}^{\circ}_{25}(relative) - 5.0 \cdot z \tag{18}$$

Criss and Cobble (1964a,b) reported the accuracy of their expression to within ±0.5 cal mol^{-1} K^{-1} for simple ions up to 150°C. Table 6 summarizes the entropy

coefficients: $a(t)$ and $b(t)$. Table 7 gives the absolute partial molar entropies of selected ions at various temperatures.

Table 6. Summary of Entropy Coefficients for Equation (17) [cal mol^{-1} C^{-1}]

Temp	Simple Cations		Simple Anions & OH$^-$		Oxy anions		Acid oxy anions		Std. State (Entropy of H+(aq))
t, °C	a(t)	b(t)	a(t)	b(t)	a(t)	b(t)	a(t)	b(t)	
25	0	1	0	1.000	0	1.000	0	1.000	-5.0
60	3.9	0.955	-5.1	0.969	-14.0	1.217	-13.5	1.380	-2.5
100	10.3	0.876	-13.0	1.000	-31.0	1.476	-30.3	1.894	2.0
150	16.2	0.792	-21.3	0.989	-46.4	1.687	(50.0)	(2.381)	6.5
200	(23.2)	(0.711)	(30.2)	(0.981)	(67.0)	(2.020)	(70.0)	(2.960)	(11.1)

Source: Criss and Cobble (1964a)

Table 7. Absolute Partial Molar Entropies of ions at Infinite Dilution [cal mol^{-1} C^{-1}]

Ion	25 °C	60 °C	100 °C	150 °C	200 °C
H$^+$	-5.0	-2.5	2.0	6.5	11.1
Li$^+$	-2.0	2.3	8.3	14.2	...
Na$^+$	9.0	13.3	18.8	23.7	...
K$^+$	20.0	22.1	27.1	23.0	...
MG^{+2}	-33.0	-32.6	-23.4	-14.1	...
Ba^{+2}	-7.7	-3.0	4.4	10.9	...
F$^-$	1.7	-2.3	-9.4	-18.6	...
Cl$^-$	18.5	12.6	5.2	-3.2	-0.8
Br$^-$	24.7	18.7	11.2	2.7	4.9
I$^-$	31.6	25.1	18.3	...	...
OH$^-$	2.4	-3.2	-11.2	-19.7	-16.3
ClO^{4-}	48.5	50.6	45.9	...	...
NO^{3-}	40.0	35.2	28.9	...	...
SO$_4^{2-}$	14.8	1.9	-11.2	-25.3	-32.5

Source: Criss and Cobble (1964a)

Heat Capacity Estimation Techniques

Criss and Cobble (1964a,b) then extended their work to include a correlation between the entropy correspondence principle of an ion at two known or predicted temperatures to the average value of the heat capacity between the temperature range for different classes of ions.

$$\bar{C}_{p_2}^{\circ}\Big|_{25}^{t_2} = \frac{\bar{S}_{t_2}^{\circ} - \bar{S}_{25}^{\circ}}{\ln T_2 / 298.2} \tag{19}$$

Combining equations (17) and (19)

$$\bar{C}_{p_2}^{\circ}\Big|_{25}^{t_2} = \frac{a(t) - \bar{S}_{25}^{\circ}\left[1.000 - b(t)\right]}{\ln T_2 / 298.2} \tag{20}$$

which can be written as

$$\bar{C}_{p_2}^{\circ}\Big|_{25}^{t_2} = \alpha(t_2) - \beta(t_2) \cdot \bar{S}_{25}^{\circ} \tag{21}$$

where

$$\alpha(t_2) = \frac{a(t)}{\ln T_2 / 298.2}$$

$$\beta(t_2) = \frac{-\left[1.000 - b(t)\right]}{\ln T_2 / 298.2}$$

Table 8 below summarizes heat capacity coefficients: $\alpha(t_2)$ and $\beta(t_2)$. Table 9 gives the ionic partial molar heat capacity of selected ions at various temperatures.

Table 8. Summary of Heat Capacity Coefficients

Temp	Simple Cations		Simple Anions & OH⁻		Oxy anions		Acid oxy anions		$\bar{C}_{p_{H^+}}^{\circ}\Big|_{25}^{t_2}$
t, °C	$\alpha(t)$	$\beta(t)$	$\alpha(t)$	$\beta(t)$	$\alpha(t)$	$\beta(t)$	$\alpha(t)$	$\beta(t)$	
60	35	-0.41	-46.0	-0.280	-127.0	1.960	-122.0	3.440	23.0
100	46	-0.55	-58.0	0.000	-138.0	2.240	-135.0	3.970	31.0
150	46	-0.59	-61.0	-0.030	-133.0	2.270	-143.0	3.950	33.0
200	50	-0.63	-65	-0.04	-145.0	2.530	-152.0	4.240	35.0

Source: Criss and Cobble (1964a)

Table 9. Ionic Partial Moral Heat Capacity for Selected Ions [cal mol⁻¹ C⁻¹]

Ion	$\bar{C}^{\circ}_{P_{H^+}}\big|_{25}$	$\bar{C}^{\circ}_{P_{H^+}}\big|^{60}_{25}$	$\bar{C}^{\circ}_{P_{H^+}}\big|^{100}_{25}$	$\bar{C}^{\circ}_{P_{H^+}}\big|^{150}_{25}$	$\bar{C}^{\circ}_{P_{H^+}}\big|^{200}_{25}$
H⁺	28	23	31	33	35
Li⁺	41	36	47	47	52
Na⁺	37	35	41	41	45
K⁺	31	27	35	35	39
MG⁺²	62	51	67	69	75
Ba⁺²	44	38	50	50	55
F⁻	-57	-47	-58	-61	-65
Cl⁻	-59	-51	-58	-62	-66
Br⁻	-61	-53	-58	-61	-65
I⁻	-62	-55	-58	-61	-64
OH⁻	-57	-47	-58	-61	-65
CIO⁴⁻	-40	-33	-36	-39	-39
NO³⁻	-56	-49	-63	-55	-57
SO₄²⁻	-115	-99	-108	-105	-144

Source: Criss, C. M. and Cobble, J. W. (1964a)

If we evaluate the correspondence relationship (equation (21) as the temperature interval approaches unity:

$$\lim_{\Delta t \to 1} \bar{C}^{\circ}_{P_2}\big|^{t_2}_{25} \to \bar{C}^{\circ}_{P_2}(t) \tag{22}$$

The above equation suggests that the estimation of point values of the ionic heat capacity at a given mean temperature given below:

$$\bar{C}^{\circ}_{P_2}(t) \approx A(t) - B(t) \cdot \bar{S}^{\circ}_{25} \tag{23}$$

where

$\bar{C}^{\circ}_{P_2}(t)$ = absolute reference ($\bar{C}^{\circ}_{P_2(H^+, aq.)} \equiv 28$ cal mol⁻¹ C⁻¹) ionic heat capacity at 25°C,

$A(t), B(t)$ = heat capacity coefficients (Simple cations, Na+; simple anions, OH-; oxy anions; acid oxy anions; and H+) at various temperatures.

Table 10 gives mean heat capacity coefficients at 25°C: $A(t)$ and $B(t)$.

Table 10. Summary of Mean Heat Capacity Coefficients at 25°C

Ion:	A	B
Cations	41.6	-0.52
Simple Anions & OH-	-56.5	0.18
Oxy anions	-145	2.20
Acid oxy anions	-136	3.07

Source: Criss and Cobble (1964a)

Criss and Cobble (1964a,b) suggested the following reasons for the positive heat capacities for cations and the negative heat capacities for anions:

1. The temperature dependence of the Born equation to the contribution of the dielectric term may be changing sign.

2. The temperature hydration effects of cations and anions

Criss and Cobble concluded that the present ionic heat capacity divisions are in qualitative agreement with those obtained from purely theoretical reasons from previous researchers, but the question can probably be resolved by repetition of thermo cell experiments at higher temperatures.

Results

We estimated the partial molar entropy at infinite dilution at 25°C for piperazine constituents (PZH^+, $PZCOO^-$, H^+PZCOO^-, $PZ(COO^-)_2^{-2}$) from the Powell and Latimer relation, equation (15). For this estimation, we assumed the effective ionic radius for the piperazine constituents equal to 3 Å. Aspen Plus Physical Property Database assigns an effective ionic radius equal to 3 Å for all ionic species. The following data summarizes these results:

Table 11. Partial Molar Entropy at Infinite Dilution at 25°C from the Powell and Latimer Relation [cal mol⁻¹ C⁻¹]

Ion:	Charge	MW	$\bar{S}_{25}^\circ(rel.)$	$\bar{S}_{25}^\circ(abs.)$
PZH+	1	87.15	12.78	17.78
H+PZCOO-	0	130.15	43.30	43.30
PZCOO-	-1	129.14	73.29	68.29
PZ(COO-)2	-2	172.14	103.66	93.66

Source: This work followed the treatment of H^+PZCOO^- from Bishnoi (2000), who treated the ion as a cation.

We estimated the partial molar entropy at infinite dilution at elevated temperatures for piperazine ionic constituents (PZH^+, $PZCOO^-$, H^+PZCOO^-, $PZ(COO^-)_2^{-2}$) from the Criss and Cobble relation, equation (17). The following data summarizes these results:

Table 12. Partial Molar Entropy at Infinite Dilution at Various Temperatures from the Criss and Cobble Relation [cal mol⁻¹ C⁻¹]

Ion	Charge	Relative Reference Partial Molar Entropy					Absolute Reference Partial Molar Entropy				
		25 °C	60 °C	100 °C	150 °C	200 °C	25 °C	60 °C	100 °C	150 °C	200 °C
PZH+	1	12.78	73.38	23.88	23.78	24.74	17.78	20.88	25.88	30.28	35.84
H+PZCOO-	1	13.30	23.88	24.33	24.20	25.11	18.30	21.38	26.33	30.70	36.21
PZCOO-	-1	73.29	66.61	71.80	75.31	216.05	68.29	69.11	69.80	68.81	204.95
PZ(COO-)2	-2	103.66	94.99	111.25	124.61	278.40	93.66	99.99	107.25	111.61	256.20

Source: This work followed the treatment of H^+PZCOO^- from Bishnoi (2000), who treated the ion as a cation.

We estimated the mean heat capacity at infinite dilution at 25°C for piperazine ionic constituents (PZH^+, $PZCOO^-$, H^+PZCOO^-, $PZ(COO^-)_2^{-2}$) from the Criss and Cobble relation, equation (23). The following data summarizes these results:

Table 13. Mean Heat Capacity at Infinite Dilution at 25°C from the Criss and Cobble Relation [cal mol⁻¹ C⁻¹]

Ion:	Charge	MW	$\bar{S}^\circ_{25}(abs.)$	$\bar{C}^\circ_{P_2}(t)$
PZH+	1	87.15	17.78	50.90
H+PZCOO	1	130.15	18.30	51.17
PZCOO-	-1	129.14	68.29	-295.24
PZ(COO-)	-2	172.14	93.66	-351.06

Source: This work followed the treatment of H^+PZCOO^- from Bishnoi (2000), who treated the ion as a cation.

We estimated the partial molar heat capacity at infinite dilution at elevated temperatures for piperazine ionic constituents (PZH^+, $PZCOO^-$, H^+PZCOO^-, $PZ(COO^-)_2^{-2}$) from the Criss and Cobble relation, equation (21). Table 14 summarizes these results.

Table 14. Partial Molar Heat Capacity at Infinite Dilution at Elevated Temperatures from the Criss and Cobble Relation [cal mol^{-1} C^{-1}]

Ion	Charge	$\bar{S}_{25}^{\circ}(abs.)$	Absolute Partial Molal Heat Capacity				
			25 °C	60 °C	100 °C	150 °C	200 °C
PZH+	1	17.78	50.90	42.29	55.78	56.49	61.20
H+PZCOO-	1	18.30	51.17	42.50	56.07	56.80	61.53
PZCOO-	-1	68.29	-295.24	-260.85	-290.97	-288.02	-317.78
PZ(COO-)2	-2	93.66	-351.06	-310.58	-347.81	-345.62	-381.97

Source: This work followed the treatment of H^+PZCOO^- from Bishnoi (2000), who treated the ion as a cation.

A correlation diagram of the mean heat capacity vs. the absolute partial molar entropy at infinite dilution at 25°C given below in Figure 6 illustrates the accuracy of the estimating correlations for the piperazine ionic constituents as compared to other monatomic ions.

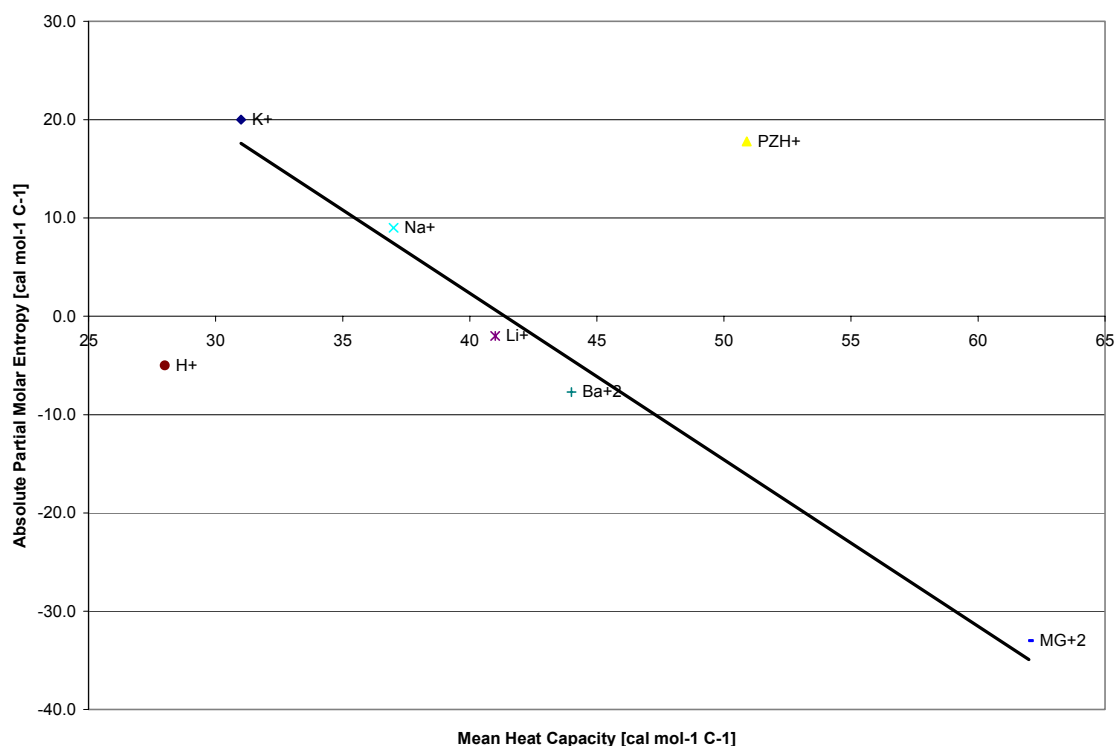**Figure 6. Absolute Partial Molar Entropy and Mean Heat Capacity at Infinite Dilution at 25°C [cal mol-1 C-1] for Specified Cations**

Source: This work followed the treatment of H^+PZCOO^- from Bishnoi (2000), who treated the ion as a cation.

The departure from a linear relationship for the piperazine ionic constituents could be explained by the estimation technique employed. The Powell and Latimer correlation model accurately describes the entropy of monatomic ions but for cyclic ring structure of piperazine ions, the departure from a linear relationship was magnified.

Conclusions

The Powell and Latimer Correlation for the estimation of the partial molar entropy at infinite dilution at 25°C as compared to the Criss and Cobble Correlation for the estimation of the mean heat capacity at infinite dilution at 25°C for piperazine ionic constituents did not accurately describe the linear relationship that exists between the two quantizes.

Recommendations and Future Work

One recommendation for future work is to expand the above results to include the Laidler Correlation for the estimation of the partial molar entropy at infinite dilution. His correlation, based on the univalent radii of Pauling, could offer a closer fit to the linear relationship between entropy and heat capacity.

Second, the literature search should be expanded to include other estimation methods for more complex ions. We feel that the Criss and Cobble Correlation is accurate for extrapolating the entropy and heat capacity to higher temperatures, but the need for an accurate model to describe physical properties for infinite dilution at 25°C needs further study.

Subtask 1.3 – Develop Integrated Absorber/Stripper Model – ACM Model for Stripper

by Babatunde Oyenekan
(Supported by this contract)

We have initiated development of a stripper model in Aspen Custom Modeler (ACM). ACM is a high-level mathematical tool used to represent and solve systems of algebraic and differential equations. It can call Aspen Plus property tools and can be incorporated as a block into an Aspen Plus model.

ACM should be superior to RateFrac in its ability to simulate the stripper. RateFrac is not ideally suited to deal with the fundamental process of desorption with very fast reaction that will dominate the behavior of stripper mass transfer. We can simulate this behavior rigorously in ACM by attaching the Bishnoi FORTRAN code for integrating mass transfer with reaction in the boundary layer.

Babatunde Oyenekan has been learning the methods of ACM. In the next reporting period he will develop a model of the stripper in this framework.

Task 2 – Pilot Plant Testing

Subtask 2.1 – Pilot Plant Test Plan – Development of Analytical Methods

by Terraun Jones
(Supported by other industrial sponsors)

Introduction

Monoethanolamine (MEA) and piperazine are amines that have been proposed for use in aqueous scrubbing for CO_2 capture from flue gas. Liquid analysis techniques are required to determine operating concentrations of these amines and their degradation products. This paper will show revised gas chromatography methods devised for alkanolamines, piperazine, and possible amine products that result from oxidative degradation of the solutes and quantify entrainment and evaporation for piperazine degradation in promoted potassium carbonate solutions. It will also show results from charging several solutions with hydrogen peroxide to find degradation products.

Gas Chromatography

Method Setup

The Gas Chromatograph is an HP 5890 with an HP 7673 Autoinjector. The column is an HP-5 capillary column that is 30 meters and has a .53mm and 1.5μm lining. The system is a split/splitless injector with helium as the carrier gas. The split ratio is the ratio of column gas rate to overall gas rate, which is 20, with column gas rate of 10ml/min. All of this is checked with a bubble flow meter. The rest of the gas is vented. The split is designed to lessen the work load on the column for separations by diluting the vaporized solution. air, hydrogen, and a makeup gas of helium are used for the FID detector for better peak detection. The air rate is 400ml/min. The hydrogen rate is 30ml/min and the makeup gas rate is 10ml/min.

The temperature ramping system was optimized to achieve separation of components that come out close together and still keep the sharpness of the peaks. The run time is 15 minutes. The first five minutes run isothermally at $40^{\circ}C$. The temperature is then ramped up to $190^{\circ}C$ at $15^{\circ}C$/min. The injector and detector are set at $180^{\circ}C$ so we do not achieve thermal degradation of the components. The system is computer automated with Galaxie Chromatogram software, which fully controls the injection and detection process.

Results

Figure 7 shows a sample solution of MEA, piperazine, diethanolamine (DEA), ethylenediamine (EDA), hydroxyethyl-ethylenediamine (HEEDA) and imidazolidinone (IMI, also known as ethylene urea) and water with roughly equal mass analyzed by GC. The first peak at 1.1 minutes is ethanol, which is used for internal standard calibration. The EDA comes out first with the top of the peak coming out at 2.7 minutes. MEA immediately comes out after with the peak coming at around 3.1 minutes. Piperazine came out at 7.6 minutes. HEEDA came out at 10.3 minutes, DEA came out at 10.7

minutes and IMI came out at 13.8. EDA and MEA, which have similar molecular weights (60.10 and 61.71 grams/mole, respectively) were separated well, even at 20 wt% of each. HEEDA and DEA also have similar molecular weights (104.2 and 105.1 grams/mole). The ramping sharpens up the piperazine (MW 86.13 grams/mole) peak. Water is not detected in the FID and therefore has no peak.
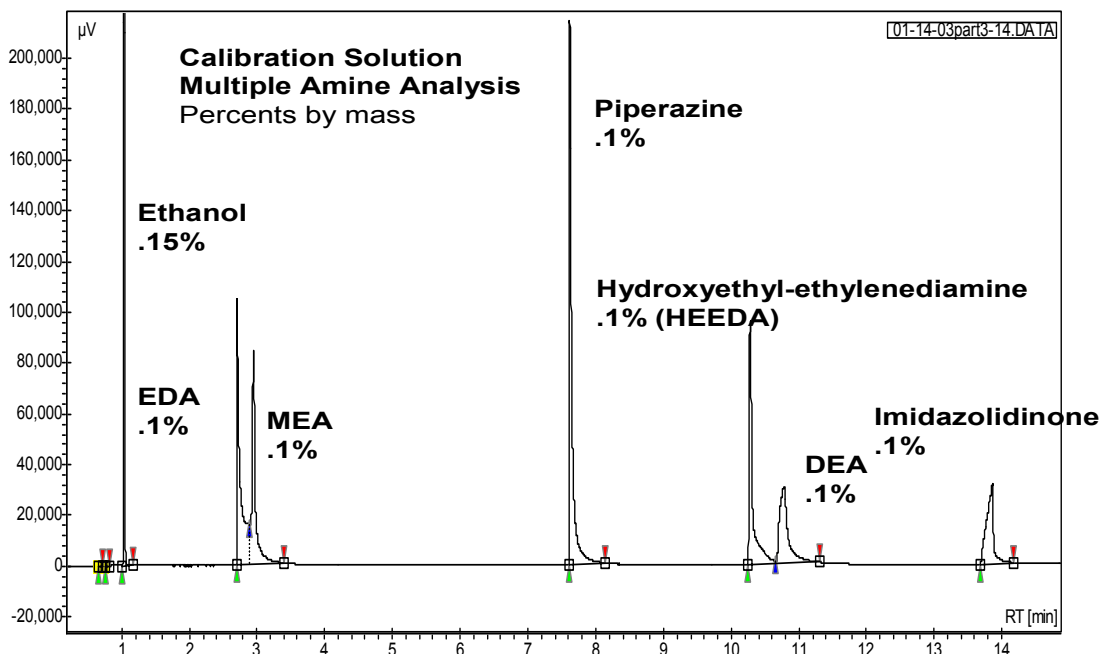

Figure 7. Gas Chromatogram for Calibration of Amines

Using this method, the components were calibrated. Figure 8 shows calibration curves for piperazine, respectively. The starting solution was diluted with water and a water/ethanol mixture to get varying wt% concentration of the amines. All components were calibrated from roughly .03 wt% to roughly .6 wt% of each. The smaller dilutions give sharper peak and better linearity for the calibration curves. The external and internal calibrations are about equally linear over the range of weight percents. Because of these results, the GC was used to analyze the solutions with confidence.

Piperazine Degradation

Experimental Setup

Air at 1L/min is mixed with CO_2 gas at 20 cc/min to make a 2% CO_2 stream. This stream is saturated at reactor temperature in a 3L water bath. The saturated air stream is sent to the reactor. The reactor is glass, jacketed, and connected to a temperature bath to regulate the temperature. A mist eliminator was added to control entrainment in the system, which will be discussed later. Syringe samples are taken once a day at approximately 24 hours intervals over 7 days. The solutions are analyzed by GC or IC for content. The volume and mass of the sample is recorded as well as the time and

the volume in the reactor. The volume of the reactor is recorded by measuring the height of the solution. These measurements account for water balances and help calculate the over mass of components in the system.

Peroxide Experiments

Since there is not a lot of information on what piperazine degrades oxidatively into, hydrogen peroxide was added to two piperazine/potassium carbonate solutions in varying amounts. Oxygen in aqueous solution usually takes the form of hydrogen peroxide, so essentially the solution is charged with oxygen. Figure 8 shows a GC readout of one of the charged solutions. There are three peaks that are currently unidentifiable. Table 15 contains molar data for piperazine and hydrogen peroxide. These solutions were analyzed by GC to analyze the components and calculate the concentrations.
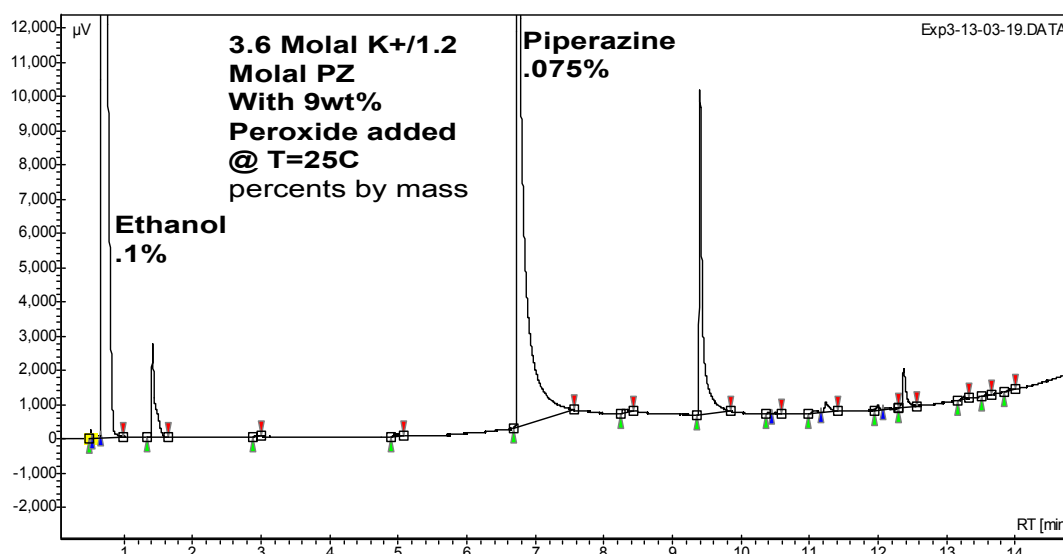
Figure 8. Gas Chromatogram for 1:1 Mole Ratio Piperazine to Hydrogen Peroxide

Table 15. Hydrogen Peroxide Results Divided by the Initial Number of Moles of Piperazine

Solution	Ratio of Moles final (ext)	Ratio of Moles Final (int)	Ratio of Moles Peroxide
3.6/1.2 T=25C	0.477	0.521	0.717
3.6/1.2 T=25C	0.509	0.494	1.071
3.6/1.2 T=64C	0.665	0.658	0.895
5.0/2.5 T=25C	0.505	0.490	0.611
5.0/2.5 T=25C	0.349	0.341	0.967

Solution	Ratio of Moles final (ext)	Ratio of Moles Final (int)	Ratio of Moles Peroxide
5.0/2.5 T=57C	0.977	0.950	0.583

Results

Overall Piperazine Loss

Figure 9. GC Readout for Solution Analyzed with Current Temperature Ramp

Using GC, degraded piperazine solutions were analyzed. These solutions contain potassium bicarbonate at high concentration and iron at low concentration. These solutions are diluted to prevent clogging due t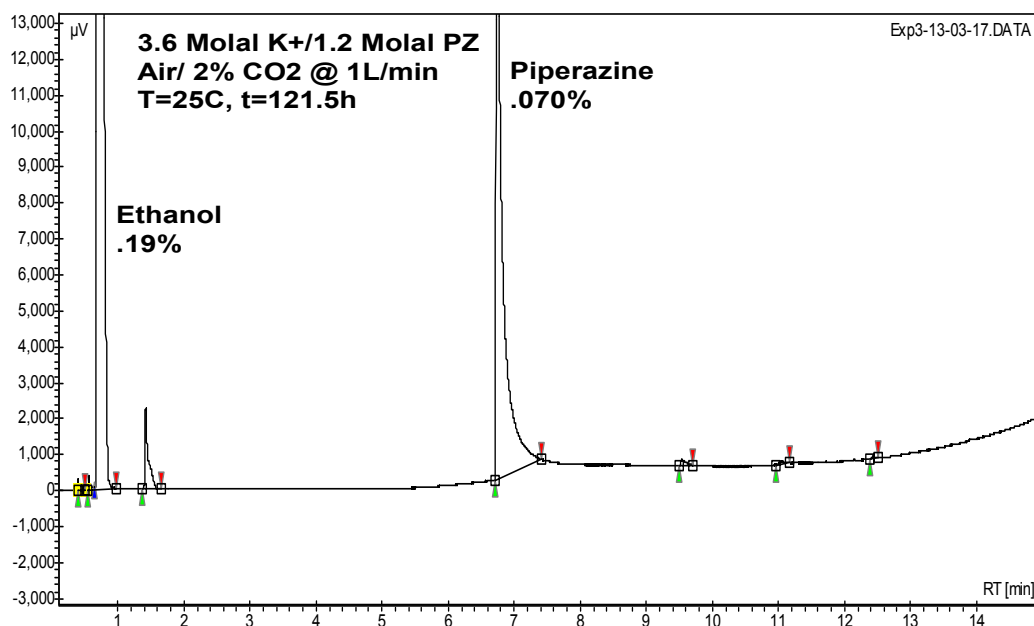o salt collection. After the weight percents are found, the concentration is calculated. The concentrations in the figures are not the actual concentrations in the reactor, but the molar mass of the species divided by the original volume of solution in the reactor. This is done because it is assumed that volume changes in the reactor are due to water either being evaporated or put in. Equation 17 is used for calculating concentration.

$$\text{Conc}\left(\frac{\text{mol}}{\text{L initial solution}}\right) = \frac{\text{wt\%}_{analyte}\ \rho_{sample}\ V_{rxter}}{MW_{amine}\ V_{initial}} \tag{17}$$

It is assumed that since the samples are diluted and rapidly heated, all carbamates are returned to the original amines. Of great importance is that the same peaks that appear in the peroxide experiment appear in the reaction chromatogram.
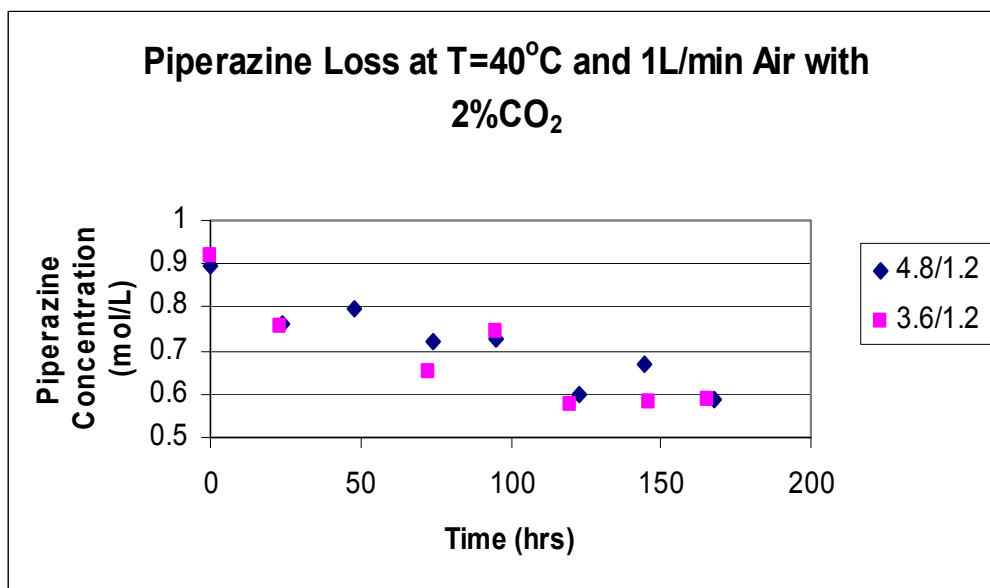
Figure 10. Piperazine Loss for Two Experiments

Piperazine was plotted for two experiments. The experiments are 3.6 Molal KHCO3/1.2 Molal piperazine and 4.8 Molal KHCO3/1.2 Molal piperazine. The rate of piperazine loss for 3.6/1.2 is 1.8 mM/hr, and for 4.8/1.2 is 2.0 mM/hr over the course of the experiment. These loss rates are similar to loss rates that were discussed in the previous paper. This could mean the rate is only as good as the dissolution of oxygen into solution, which is a mass transfer controlled process.

Evaporation and Entrainment

If the rate of piperazine disappearance will be used to characterize degradation, it is important to quantify all the ways piperazine can leave the reactor system. Since a continuous flow rate of gas is bubbling into the reactor and leaving the system for an extended period of time, evaporation and entrainment can become significant. Preliminary evaporation data shows as high as a 10ppm concentration of piperazine in the gas phase over highly concentrated piperazine solutions with no salt present. Adding potassium salt will lower the concentration in the gas phase. Using 10ppm as a ceiling for evaporation, the evaporation rate was calculated to be .077 mM/hr, or roughly 4% of the overall piperazine loss. As the piperazine concentration decreases and the potassium increases, this number can go down as much as 80%, making it insignificant in the overall loss in the system.
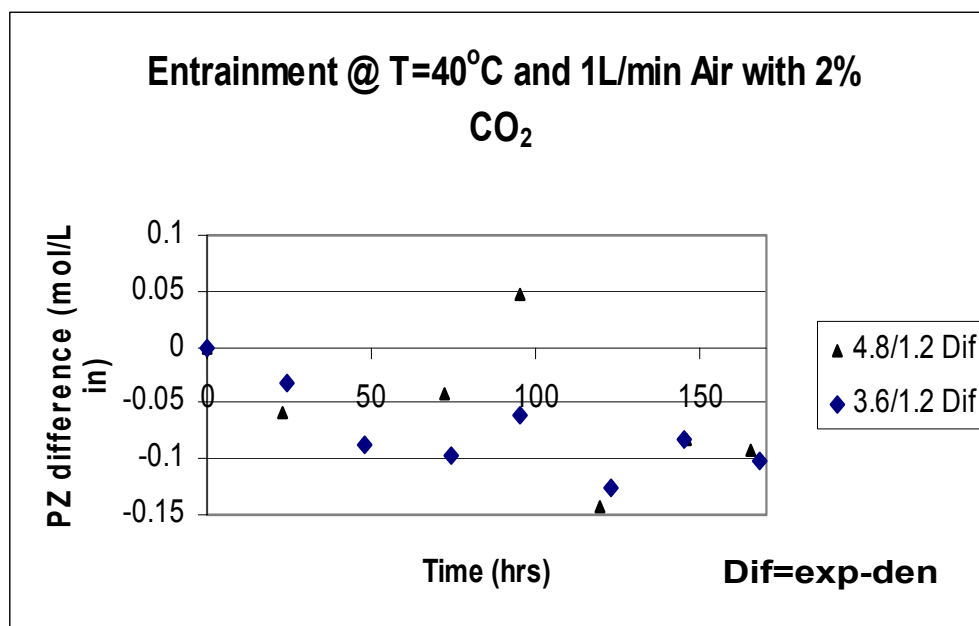
Figure 11. Entrainment Calculated for Each Experiment

Entrainment appears to be a much more significant source of piperazine loss than evaporation. Figure 11 shows a quantified chart of entrainment each day. The calculation is done based on density correlations. Density is a strong function of potassium ion concentration, but a weak function of piperazine concentration (Cullinane, 2002). Concentrations were calculated using density if there is only dilution due to water. If this concentration is greater than the concentration calculated from the experimental density, the change is due to entrainment. Based on this, the calculated entrainment rate for 3.6/1.2 is .60 mM/hr and for 4.8/1.2 is .57 mM/hr. This was before a mist eliminator was added to the experimental apparatus. The mist eliminator should decrease the entrainment in the system.

Conclusions and Recommendations

The GC temperature ramping system was changed from a previous experiment to detect peaks at small levels and achieve better separation. It is also for compounds that elude at late times. An experiment using hydrogen peroxide to charge solutions with oxygen yield a roughly 1:1 ratio of piperazine disappearance to oxygen in the system and yield degradation product peaks seen in experiments. Entrainment is roughly 30% of the overall loss of piperazine and evaporation is relatively insignificant is the system. The resulting degradation rate is 1.1 mM/hr for 3.6/1.2 and 1.3 mM/hr for 4.8/1.2 over the course of the experiment. The resulting degradation rates still show a loss of piperazine being roughly the same as other commonly used alkanolamines for acid gas scrubbing. To better measure entrainment, ion chromatography to measure potassium ion concentration or any other method is better suited.

Future Work

Piperazine degradation will be further studied. The extra components from the degradation will be identified through GC/MS or NMR. Solutions of differing piperazine and potassium carbonate concentrations will be degraded, in particular, solutions of interest to the upcoming pilot plant work. Temperatures seen in acid gas scrubbers will be used. Metals such as iron, usually resulting from the corrosion of carbon steel, and vanadium, a commonly used corrosion inhibitor in potassium carbonate solutions, will be studied to understand their effects on oxidative degradation. The analysis methods utilized for degradation will also be extended to upcoming pilot plant research on these solutions.

Subtask 2.2 – Design, Modifications, Order Equipment and Packing Materials

by Eric Chen
(Supported by this contract)

Project Management

In this quarter, all efforts were focused on the CO_2 capture pilot project. A Gantt chart was developed to help facilitate the management of the project and to clearly identify project milestones. Bi-monthly meetings were established to ensure that tasks were completed according the project schedule. A critical path analysis was also performed. The tentative start-up date for the pilot plant is slated for the beginning of November 2003. The official commencement of Campaign 1 will be contingent on the initial operational difficulties encountered during the troubleshooting phase of the pilot plant start-up.

Heat Exchangers

The design for the absorber solvent cooler and the stripper feed heater has been completed. Two Brown Fintube heat exchangers were donated by Huntsman Chemical. The twin U-tube heat exchangers each have a surface area of 107 ft^2, 1" OD tubes, 3" shells, and 15/16" longitudinal fins. A visit to the Huntsman site in Austin was conducted to survey the piping connections of the exchangers and to encourage the displacement of the heat exchangers from the Huntsman site. The exchangers were delivered to the University of Texas Separations Research Program (UT-SRP) site towards the latter part February. After some difficulty, exchanger drawings were obtained from a local distributor and then it was determined that only the tube side was constructed from stainless steel. The shell side of the heat exchangers was constructed of carbon steel. Due to pressure drop concerns, the corrosive process stream would need to be on the shell side. Also, it was determined that the heat transfer area was not adequate for use as the solvent cooler. Therefore, a new solvent cooler was designed and ordered. A new heat exchanger was ordered from ITT Standard. The exchanger is constructed

from 316 stainless steel and has an area of 144 ft^2. The exchanger should be onsite by the end of April. Cooling water at 50°F will be used to cool the process fluid.

After performing some pressure drop calculations, it was decided to use the two Huntsman exchangers in parallel as the solvent heater for the stripper feed. Steam at 135 psi will be used to heat the solvent. The solvent heater will need to be strictly controlled to minimize piperazine degradation. The solvent cooler and heaters will be mounted on a rack support system to centralize operational procedures and to minimize the footprint. The rack is currently in the design phase.

Air Cooler

The outlet gas of the absorber column will need to be cooled before it can be recycled back into the column. An air cooler was sized to remove approximately 390,000 BTU/hr. An estimate of heat load from the heat of absorption of CO_2 in the solvent was determined to be about 280,000 BTU/hr. It was assumed that approximately half of this heat load will be carried out by the solvent and that the remaining heat load will be converted into latent energy resulting in saturation of the gas with water. An air cooler from Super Radiator Coils was ordered. The air cooler is constructed from 316 stainless steel and should be on-site by the end of May. Cooling water at 50°F will be used to cool the process gas.

Process Instrumentation

The flow rate, temperature and density of the solvent stream will be measured by a Micro Motion® Coriolis flow meter. The flow meter is manufactured by Emerson Process. We are in the process a negotiating an academic discount with the manufacturer and hope to procure a total of 4 flow meters. The Micro Motion® flow meters will be mounted on the same rack as the three heat exchangers. The density measurement can be used to maintain the water balance in the system. One flow meter will be located downstream of the absorber feed tank and another flow meter will be located just upstream of the stripper inlet. A temperature profile will be generated for the absorber column to characterize the temperature bulge. Temperature measurements will be conducted using up 20 thermocouples and 4 thermocouples in the absorber and stripper columns, respectively. The preliminary survey shows that this should be possible without much modification to either column.

Analytical Setup

The setup for the analytical system is currently in the design phase. Two CO_2 gas analyzers have been ordered from Vaisala. The Vaisala GMT220 analyzers are designed for harsh and humid industrial applications. The CO_2 monitors will be used for process control measurements. The analyzers will measure CO_2 gas concentrations at the inlet and outlet of the absorber column. In addition, an analytical CO_2 measurement will be made with either a Horiba PIR-2000 or a portable FTIR unit. Currently there are two Horiba instruments that are available. One analyzer is being used by UT-SRP and would need to be reconfigured to operate at the higher CO_2 concentrations. There is another

Horiba instrument that has a concentration range of 0-20%, 0- 60%, and 0-100% CO_2. This instrument was found scrapped by an unknown research group and will need to be tested. Use of the FTIR would require the installation of the Modbus® protocol on the Delta V process control unit. Ultimately, the decision will be determined by the setup costs.

The decision to monitor CO_2 loading with pH measurements is still being considerded. Over the pH range of 9-12, the CO_2 loading was linear in response for a solution of 1.8 m potassium carbonate and 0.6 m piperazine at 40°C. However, due to the high concentration of electrolytes and organics, problems may occur at the junction potential and give erroneous pH measurements. Conductivity measurements performed using 0.6 M piperazine exhibited a maximum at a loading of approximately 0.7 mol CO_2/mol PZ, which also presents a problem.

Liquid analysis of the potassium and piperazine will be required to monitor any changes in the solution composition over each campaign. Ion chromatography (IC) is currently being used to analyze potassium (K^+) concentrations in our group. The analysis has a retention time of approximately 4 to 5 minutes. IC may also be used to measure piperazine concentration; however, methods have not been developed yet. Gas chromatography is currently being used by our group to measure piperazine concentration. Piperazine has a retention time of about 7 to 8 minutes.

A total carbon analyzer is also available. The concentration of CO_2 can be measured directly by the injecting phosphoric acid into the solution. The CO_2 is released as a gas and quantified by a CO_2 gas analyzer, while the organic carbon remains behind in the solution. Piperazine concentration could be obtained by performing a total carbon analysis on the solution and taking the difference between the two. High performance liquid chromatography (HPLC) is also being explored as a possible alternative to analyzing piperazine. HPLC does not have the same issues as GC, where the samples are injected at high temperatures and may result in the degradation of the analyte. HPLC does not have this problem and is currently used by Huntsman Chemical for their amine analyses.

Some other analytical methods that are being explored include: wet chemistry methods to determine total effective potassium by performing an acid/base titration, and atomic absorption (AA) or an ion-selective electrode (ISE) to measure total potassium. Additional analytes include acetate, formate, chloride, and sulfate. Total alkalinity is another parameter that may be measured.

CO_2 Delivery System

The design of the CO_2 delivery system is underway. Current market prices indicate that the cost of potassium carbonate is approximately $40 per 100 lbs, while potassium bicarbonate is approximately $80 per 100 lbs. Potassium hydroxide may also be used to charge the liquid solution. However, large amounts of CO_2 must be absorbed and the potential to overshoot the desired CO_2 loading is much greater. The cost of potassium hydroxide is approximately $52 per 100 lbs. Therefore, it will be more economical to charge the initial solution with potassium carbonate and perform additional adjustments with CO_2 gas. The options for CO_2 gas delivery include renting a large tank

or using individual gas cylinders. The amount of makeup CO_2 will ultimately depend on how well the plant is operated and the losses attributed to the vent.

Process Calculations

Using the pressure drop data for the CMR #2 generated by Ian Wilson, three constants were regressed using the Stichlmair, Bravo, and Fair (SBF) pressure drop correlation. However, the resulting fits were in some cases within 40% and therefore not acceptable. A much better fit was correlated using the Packed Bed Simulator developed by Piché et al. 2001. The simulator includes a parameter for liquid viscosity which the SBF model did not. Based on the correlations developed by Tim Cullinane for the density and viscosity, a CO_2 capacity of 0.5 m and an operating pressure drop of 1 inch/ft packing, a maximum gas rate of approximately 470 acfm (40°C, 1 atm) and a corresponding liquid rate of 39 gpm was obtained for a solvent composition of 2.5 m K_2CO_3 and 2.5 m piperazine.

Future Work

The next critical path item is the modification of the welding bid package. The original piping iso's will need to be adjusted to reflect the changes of the three new heat exchangers and of the addition of the Micro Motions[®]. Once the piping iso's have been revised, a welding bid can be submitted and all the associated materials may be purchased. The design for the analytical setup will need to be finalized and the associated equipment and materials procured. The design for the process instrumentation and temperature profile will also need to be completed and the associated parts ordered. The design of the CO_2 delivery system will also need to be completed. An economical analysis of packing materials for the absorber column will need to be commenced and finished. This will aid in the proper selection of packing material for the first campaign. The current default packing is CMR #2.

References

Aseyev, G.G. (1999). Electrolytes: Equilibria in Solutions and Phase Equilibria. Calculation of Multicomponent Systems and Experimental Data on the Activities of Water, Vapor Pressures, and Osmotic Coefficients. Begell House: New York.

Aspen Technology. (2001a). Aspen Plus: Getting Started Modeling Processes with Electrolytes, version 11.1. Cambridge: Author.

Aspen Technology. (2001b). Aspen Physical Property System: Physical Property Methods and Models, version 11.1. Cambridge: Author.

Austgen, D. (1989). A Model of Vapor-Liquid Equilibria for Acid Gas-Alkanolamine-Water Systems. Ph.D. Dissertation, The University of Texas at Austin, Austin, TX.

Bishnoi, S. (2000). Carbon Dioxide Absorption and Solution Equilibrium in Piperazine Activated Methyldiethanolamine. Ph.D. Thesis, The University of Texas at Austin, Austin, TX.

Bishnoi, S., and Rochelle, G. T. (2000). Absorption of Carbon Dioxide into Aqueous Piperazine: Reaction Kinetics, Mass Transfer, and Solubility. *Chemical Engineering Science*, 55(22), 5531-43.

Caracotsios, M. (1986). Model Parametric Sensitivity Analysis and Nonlinear Parameter Estimation. Theory and Applications. Ph.D. Dissertation, The University of Wisconsin, Madison, WI.

Chen, C., Britt, H. I., Boston, J. F., and Evans, L. B. (1982). Local Composition Model for Excess Gibbs Energy of Electrolyte Systems. *AIChE J.* 28(4), 588.

Cox, B. G., and Parker, A. J. (1973). *Journal of the American Chemical Society,* 95(21), 6879-84.

Criss, C. M. and Cobble, J. W. (1964a). The Thermodynamic Properties of High-Temperature Aqueous Solutions. IV. Entropies of the Ions up to 200° and the Correspondence Principle. *Journal of the American Chemical Society*, 86(24), 5385-90.

Criss, C. M. and Cobble, J. W. (1964b). The Thermodynamic Properties of High-Temperature Aqueous Solutions. V. The Calculation of Ionic Heat Capacities up to 200°. Entropies and Heat Capacities above 200°. *Journal of the American Chemical Society*, 86(24), 5390-93.

Cullinane, J. T. (2002). Carbon Dioxide Absorption in Aqueous Mixtures of Potassium Carbonate and Piperazine. M.S. Thesis, The University of Texas at Austin, Austin, TX.

Dean, J. A. (1992). Lange's Handbook of Chemistry. 14th ed. McGraw-Hill: New York.

Edwards, T., Maurer, G., Newman, J., and Prausnitz, J. (1978). Vapor-Liquid Equilibria in Multicomponent Aqueous Solutions of Volatile Weak Electrolytes. *American Institute of Chemical Engineers Journal*, 24(6), 966-76.

Ermatchkov, V., Kamps, A.P-S., and Maurer, G. (submitted 2002). Chemical Equilibrium Constants for the Formation of Carbamates in the System CO_2+Piperazine+Water from ^{1}H-NMR Spectroscopy. *J. Chem. Thermodyn*.

Handbook of Chemistry and Physics. 81st Ed. (2000). David R. Lide, ed. CRC Press: New York.

Horvath, A. L. (1985). *Handbook of Aqueous Electrolyte Solutions.* Chichester: Ellis Horwood, 457-71.

Kamps, A. P-S., Xia, J., and Maurer, G. (submitted 2002). Solubility of CO_2 in (H_2O+Piperazine) and in (H_2O+MDEA+Piperazine). *AIChE J*.

King, E. L. (1959). *Journal of Physical Chemistry*, 63(7), 1070-72.

Laidler, K. J. (1957). *Journal of Chemical Physics,* 27(6), 1423-24.

Pagano, J. M., Goldberg, D. E., and Fernelius, W. C. (1961). A Thermodynamic Study of Homopiperazine, Piperazine, and N-(2-Aminoethyl)-Piperazine and Their Complexes with Copper(II) Ion. *Journal of Physical Chemistry*, 65, 1062.

Piche, S., Larachi, F., and Grandjean, B. (2001). Randomly Packed Bed Simulator. Retrieved February 2003, from Universite Laval Web site: http://www.gch.ulaval.ca/~flarachi

Posey, M. L. (1996). Thermodynamics Model for Acid Gas Loaded Aqueous Alkanolamine Solutions. Ph.D. Dissertation, The University of Texas at Austin, Austin, TX.

Powell, R. E. and Latimer, W. M. (1951). The entropy of aqueous solutes. *Journal of Chemical Physics*, 19(9), 1139-41.

Renon, H., and Prausnitz, J. M. (1968). Local Compositions in Thermodynamic Excess Functions for Liquid Mixtures. *AIChE J.* 14(1), 135.

Scott, P. C., and Hugus, Z. Z. (1957). Partial molal entropies of ions in aqueous solution. *Journal of Chemical Physics*, 27(40), 461-70.

Tosh, J. S., Field, J. H., Benson, H. E., and Haynes, W. P. (1959). Equilibrium Study of the System Potassium Carbonate, Potassium Bicarbonate, Carbon Dioxide, and Water. United States Bureau of Mines, 5484.

Wulff, C. A. (1967). Entropies of the aqueous zinc(II), cadmium(II), mercury(II) and Hg22+ ions. *Journal of Chemical Engineering Data*, 12(1), 82-85.

Appendix

Scalar Parameter Nomenclature
Temperature Dependent Parameter Nomenclature

Scalar Parameter Nomenclature

API	Standard API gravity
CHARGE	Ionic Charge number (positive for cations, negative for anions)
CHI	Stiel polar factor
DGAQFM	Aqueous phase free energy of formation at infinite dilution and 25 deg C. For ionic species and molecular solutes in electrolyte systems
DGAQHG	Helgeson infinite dilution Gibbs energy of formation
DGFORM	Standard free energy of formation for ideal gas at 25 deg C
DGFVK	Parameter for the Gibbs free energy of formation. Used by the van Krevelen models
DGSFRM	Solid free energy of formation at 25 deg C
DHAQFM	Aqueous phase heat of formation at infinite dilution and 25 deg C. For ionic species and molecular splutes in electrolyte systems
DHAQHG	Helgeson infinite dilution enthalpy of formation
DHFORM	Standard enthalpy of formation for ideal gas at 25 deg C
DHFVK	Parameter for the enthalpy of formation. Used by the van Krevelen models
DHSFRM	Solid enthalpy of formation at 25 deg C
DHVLB	Enthalpy of vaporization at TB
DLWC	Vector indication diffusing or non-diffusing components for Wilke-Chang Model. Enter 1 for diffusing component or 0 or non-diffusing component.
DVBLNC	Vector indication diffusing or non-diffusing components for Chapman-Enskog-Wike-Lee Model. Enter 1 for diffusing component or 0 or non-diffusing component
HCOM	Standard enthalpy of combustion at 298.2 K
IONRDL	Riedel ionic coefficient for correction to the liquid mixture thermal conductivity of a mixture due to the presence of electrolytes
IONTYP	Ion type for the Criss-Cobble aqueous infinite dilution ionic heat capacity equation (1=cations; 2=simple anions, OH-; 3=oxy anions; 4=acid oxy anions; 5=H+)
MUP	Dipole moment
MW	Molecular weight
OMEGA	Pitzer acentric factor
OMEGHG	Helgeson Omega heat capacity coefficient
PC	Critical Pressure
RADIUS	Born radius of ionic species
RHOM	Mass density
RKTZRA	Parameter for the Rackett liquid molar volume model
S25HG	Helgeson entropy at 25 deg C
S025C	Absolute entropy at 25 deg C used in the Criss-Cobble equation for estimation of aqueous infinite dilution ionic heat capacity
S025E	Sum of element entropies at 25 deg C
SG	Standard specific gravity at 60 deg F
TB	Normal boiling point

TC	Critical temperature
TFP	Freezing point temperature
TREFHS	Reference temperature when solid reference state is used (RSTATE = 3). TREFHS is used together with DHSFRM and DGSFRM
VB	Liquid molar volume at TB
VC	Critical volume
VCRKT	Critical volume for the Rackett liquid model; defaults to VC
VLSTD	Standard liquid volume at 60 deg F
ZC	Critical compressibility factor

Temperature Dependent Parameter Nomenclature

AHGPAR   Helgeson Equation of state coefficients (for ions in the chemical reactions)

ATOMNO   Vector containing the atom types (atomic numbers) for a given molecule (e.g., H=1, C=6, O=8). Must use the vector NOATOM to define the number of occurrences of each atom.

CHGPAR   Helgeson C Heat Capacity coefficient (for ions in the chemical reactions)

CPAQ0   Aqueous phase heat capacity at infinite dilution polynomial. If no values are given then uses Criss-Cobble equation to calculate heat capacity.

CPDIEC   Pure component dielectric constant coefficients of nonaqueous solvents

CPIG   Ideal gas heat capacity

CPIGDP   DIPPR ideal gas heat capacity equation is used for most pure components

CPLXP1   Barin liquid phase heat capacity for the first temperature range

CPLXP2   Barin liquid phase heat capacity for the second temperature range

CPSDIP   Coefficients for the DIPPR solid heat capacity equation

CPSPO1   Solids heat capacity polynomial

DHVLDP   Pure component heat of vaporization coefficients for the DIPPR heat of vaporization equation

DHVLWT   Watson Heat of Vaporization equation for pure components

DNLDIP   DIPPR liquid density equation for pure components if DNLDIP is available (pure component liquid molar volume)

DNSDIP   DIPPR solid density equation

IONMOB   Coefficients for the Jones-Dole correction to liquid mixture viscosity due to the presence of electrolytes (moles)

IONMUB   Coefficients for the Jones-Dole correction to liquid mixture viscosity due to the presence of electrolytes (volume/mole)

KLDIP   Pure component liquid thermal conductivity coefficients for the DIPPR liquid thermal conductivity equation

KSPOLY   Solid Thermal conductivity

KVDIP   Pure component vapor thermal conductivity for low pressure gasses coefficients for the DIPPR vapor thermal conductivity equation

MULAND   Pure component liquid viscosity coefficients for the Andrade Liquid Viscosity equation

MULDIP   Pure component liquid viscosity coefficients for the DIPPR Liquid Viscosity equation

MUVDIP   Pure component low pressure vapor viscosity coefficients for the DIPPR Liquid Viscosity equation

NOATOM   Vector containing the number of each type of element in the component. Must be used with ATOMNO.

PCES   Parameters Estimation by the Aspen Physical Property System

PLXANT   Coefficients for the Extended Antoine vapor pressure equation for a liquid

PSANT   Pure component Coefficients for Solid Antoine vapor pressure equation

SIGDIP   Pure component liquid surface tension coefficients for the DIPPR liquid surface tension equation

VLBROC   Brelvi-O-Connell Volume Parameter

VLPO   IK-CAPE liquid density equation for pure components if VLPO is
            available (pure component liquid molar volume)
VSPOLY   Pure component coefficients for the solid molar volume equation
WATSOL   Coefficients for the water solubility equation model that calculates
            solubility of water in a hydrocarbon-rich liquid phase. This model is used
            automatically when you model a hydrocarbon-water system with free-
            water option.